Atmos. Chem. Phys. Discuss., 13, 30311–30348, 2013
www.atmos-chem-phys-discuss.net/13/30311/2013/
doi:10.5194/acpd-13-30311-2013

Atmospheric Chemistry and Physics
Discussions
Open Access

Kaolinite particles as ice nuclei: learning from the use of different types of kaolinite and different coatings

H. Wex[1], P. J. DeMott[2], Y. Tobo[2], S. Hartmann[1], M. Rösch[1], T. Clauss[1], L. Tomsche[1], D. Niedermeier[1], and F. Stratmann[1]

[1]Leibniz-Institute for Tropospheric Research, Leipzig, Germany
[2]Department of Atmospheric Science, Colorado State University, Fort Collins, Colorado, USA

Received: 12 October 2013 – Accepted: 8 November 2013 – Published: 21 November 2013

Correspondence to: H. Wex (wex@tropos.de)

Published by Copernicus Publications on behalf of the European Geosciences Union.

Abstract

Kaolinite particles from two different sources (Fluka and Clay Minerals Society (CMS)) were examined with respect to their ability to act as ice nuclei. This was done in the water subsaturated regime where often deposition ice nucleation is assumed to occur, and for water supersaturated conditions, i.e. in the immersion freezing mode. Measurements were done using a flow tube (LACIS) and a continuous flow diffusion chamber (CFDC). Pure and coated particles were used, with coating thicknesses of a few nanometer or less, where the coating consisted of either levoglucosan, succinic acid, or sulfuric acid. In general, it was found that the coatings strongly reduced deposition ice nucleation. Remaining ice formation in the water subsaturated regime could be attributed to immersion freezing, with particles immersed in concentrated solutions formed by the coatings.

In the immersion freezing mode, ice nucleation rate coefficients, j_{het}, from both instruments agreed with each other when the residence times in the instruments were accounted for. Fluka kaolinite particles coated with either levoglucosan or succinic acid showed the same IN activity as pure Fluka kaolinite particles, i.e. it can be assumed that these two types of coating did not alter the ice active surface chemically, and that the coatings were diluted enough in the droplets that were formed prior to the ice nucleation, so that freezing point depression was negligible. However, Fluka kaolinite particles which were coated with either pure sulfuric acid or which were first coated with the acid and then exposed to additional water vapor both showed a reduced ability to nucleate ice, compared to the pure particles. For the CMS kaolinite particles, the ability to nucleate ice in the immersion freezing mode was similar for all examined particles, i.e. for the pure ones and the ones with the different types of coating. Moreover, j_{het} derived for the CMS kaolinite particles was comparable to j_{het} derived for kaolinite particles coated with sulfuric acid. This is suggestive for the Fluka kaolinite possessing a type of ice nucleating surface feature which is not present on the CMS kaolinite,

ACPD

13, 30311–30348, 2013

and which can be destroyed by reaction with sulfuric acid, which might be potassium feldspar.

1 Introduction

Ice in clouds is a research topic which has received interest already before the 1950' (see e.g. Vonnegut, 1947). Despite many decades which have gone by since scientists started to work on ice in clouds, our understanding of even the basic related processes is still incomplete (Murray et al., 2012). In the atmosphere, ice containing clouds (meaning both pure ice clouds and mixed phase clouds) play important roles. They cover a significant fraction of the Earth at any time and hence influence radiative processes and also the formation of precipitation. Of the latter, the majority is produced via the ice phase in mixed phase clouds, particularly outside of the tropics.

The first step on the way to having ice in clouds is ice formation, and therefore this process is of large interest. It is known that ice can form by primary or secondary processes, an example for the latter being e.g. rime-splintering (Hallett and Mossop, 1974). The primary processes are either homogenous or heterogenous ice nucleation, where heterogeneous ice nucleation involves ice nuclei (IN) which lower the energy barrier that has to be overcome to form a stable ice cluster. Mixed phase clouds form at temperatures above those for which homogenous ice nucleation can occur. And as these clouds are also the ones responsible for forming much of the globally occurring precipitation, the heterogenous ice nucleation mechanisms are of particular interest. Additionally, it has been claimed that maybe even for cirrus clouds, heterogenous formation mechanisms might be of large importance (Spichtinger and Cziczo, 2010; Cziczo et al., 2013).

There are different pathways for heterogenous freezing, i.e. immersion, condensation and contact freezing and deposition ice nucleation. For mixed phase clouds, it has been stated that immersion freezing is the most important ice forming mechanism (Ansmann et al., 2009; Wiacek et al., 2010; de Boer et al., 2011), while for cirrus clouds

ACPD
13, 30311–30348, 2013

deposition ice nucleation and condensation/immersion freezing are considered as ice forming mechanisms, too. The differentiation between condensation and immersion freezing is often blurry, and particularly for condensation freezing different definitions have been made over the years (see e.g. Pruppacher and Klett, 1997; Hoose and Möhler, 2012; Vali, 1985). In our study, we will use the term immersion freezing for all cases when an insoluble particle is immersed in a diluted droplet. Condensation freezing will denote the case when an insoluble particle is immersed in a concentrated solution (i.e. in the case of haze particles), which principally can occur for $S_w < 1$ as long as the deliquescence RH of the soluble material which was on the insoluble core prior to forming a solution is overcome. This is similar to the "immersion freezing of solution droplets" from Hoose and Möhler (2012) or e.g. to a term called "deliquescent-heterogenous freezing" in Khvorostyanov and Curry (2004). For the fourth heterogenous ice nucleation process, contact freezing, little data is available, but new results on this topic are currently emerging as e.g., in Hoffmann et al. (2013).

Much has been learned about the nature of IN (see the two reviews given by Hoose and Möhler (2012) and Murray et al., 2012). However, on a process scale, it is still not known what exactly it is that makes a particle act as IN. Mineral dust particles are known to be an important IN source in the atmosphere (e.g., DeMott et al., 2003; Sassen et al., 2003; Cziczo et al., 2004; Hoose and Möhler, 2012; Murray et al., 2012; Atkinson et al., 2013). Deserts and also top soils of the Earth are abundant sources for mineral dust, and the respective aerosol is distributed world wide, with a stronger abundance in the Northern Hemisphere (Atkinson et al., 2013; Burrows et al., 2013, see e.g.). Different minerals have been examined with respect to their role as IN (see the summary in Murray et al., 2012), among them atmospherically relevant minerals like clay and feldspar and also quartz. Quartz generally is assumed to not be a good IN, while silicates generally are ice active (see e.g. Archuleta et al., 2005; Kanji et al., 2008; Zimmermann et al., 2008; Welti et al., 2009), and e.g. Sullivan et al. (2010a) and Niedermeier et al. (2011) explicitly mentioned that it might be the aluminosilicate minerals which are the most efficient ice active component in the test dust examined

ACPD
13, 30311–30348, 2013

in their studies (Arizona Test Dust). Recently it has been proposed that the potassium feldspar content may play the most important role for the IN ability of mineral dusts worldwide (Atkinson et al., 2013).

A uniform description or parameterization which would enable an easy incorporation of the heterogenous freezing processes in models still needs to be developed, if this will be possible at all. Understanding the processes underlying the freezing and learning about the nature of IN can help shed light onto this. Particularly for the deposition ice nucleation, the review by Hoose and Möhler (2012) shows that reported onset temperatures scatter over a large range with respect to both observed temperature and water vapor saturation ratios. Some of this scatter can be explained by different thresholds, i.e. by different frozen fractions, that were reported for the different measurements which have been included in the comparison or by other issues specific to the different instruments. However, open issues remain for the understanding of heterogeneous ice nucleation. A new suggestion concerning deposition ice nucleation was recently discussed in Marcolli (2013), viewing this particular heterogenous ice nucleation mode as either homogeneous or as immersion freezing in pores and cavities. A part of this present study will be devoted to a related discussion. It has been already described that coatings, particularly of sulfuric acid, on mineral dust particles containing aluminium-silicates can largely reduce their ice nucleation ability for deposition ice nucleation (e.g. in Archuleta et al., 2005; Cziczo et al., 2009; Eastwood et al., 2009; Sullivan et al., 2010b; Tobo et al., 2012), and for immersion freezing (e.g. Zuberi et al., 2002; Koop and Zobrist, 2009; Niedermeier et al., 2010; Sullivan et al., 2010b; Niedermeier et al., 2011; Tobo et al., 2012). However, a coating of nitric acid inhibited deposition ice nucleation for relative humidities below $\sim 97\,\%$ but not for immersion freezing (Sullivan et al., 2010a), and the observed sharp increase in ice nucleation ability at $\sim 97\,\%$ was interpreted as a change in the heterogenous ice nucleation mode, namely from deposition ice nucleation to condensation/immersion freezing. In the present study, we will explicitly show that the ice nucleation for some coated mineral dust particles can be described as immersion freezing, with the mineral dust particle being immersed in a concentrated solution for which then a freezing point depression has to be assumed.

In the present work we will show results for heterogenous ice nucleation measured with either LACIS (Leipzig Aerosol Cloud Interaction Simulator) in its immersion freezing mode (Hartmann et al., 2011) and a CFDC (Continuous flow Diffusion Chamber, Rogers et al., 2001; DeMott et al., 2010) measuring both, deposition ice nucleation and condensation/immersion freezing. Examined particles consisted of two different kaolinites with and without coatings (details are described in Sect. 2). In all cases, size segregated particles were examined.

A subset of the data presented here was already shown in Tobo et al. (2012), where data from the CFDC for Fluka kaolinite particles (pure and coated with H_2SO_4 or levoglucosan) were described. It was found that both coatings reduced the IN ability for the deposition ice nucleation while only the H_2SO_4 coating reduced the IN ability for condensation/immersion freezing in the CFDC. Therefore the levoglucosan coating was similar in its effect than nitric acid in Sullivan et al. (2010a) in inhibiting deposition ice nucleation but allowing for condensation/immersion freezing once the coating is dissolved at relative humidities close to 100 %.

The present study extends from Tobo et al. (2012). It includes a comparison of the measured immersion freezing by LACIS and the CFDC, additional data on CMS kaolinite and also data on coatings with succinic acid. Furthermore, it discusses a model for describing the heterogeneous ice formation of particles with sufficiently thick coatings at relative humidities close to 100 %, interpreting this type of freezing as immersion freezing of IN immersed in concentrated solutions.

2 Samples, set-up and instrumentation

In this study, two different kaolinites were examined. The samples were provided by Fluka and by the Clay Minerals Society (CMS, KGa-1b). In general, kaolinite belongs to the group of clays, consists largely of aluminium-silicates, and occurs in atmospheric

ACPD
13, 30311–30348, 2013

samples in amounts on the order of a few up to a few 10 % (see Murray et al., 2012). However, the Fluka kaolinite additionally contains about 5 % of potassium feldspar, while CMS kaolinite does not contain a detectable amount (Atkinson et al., 2013).

Besides pure, also coated particles were studied, where the coatings consisted of either sulfuric or succinic acid or levoglucosan. Sulfuric acid is known to be a reactive substance with the potential to decrease the IN ability of dust particles, as mentioned above. It is of atmospheric relevance as atmospheric SO_2 can be oxidized to H_2SO_4 during wet phase chemistry. Succinic acid was chosen as it is a slightly soluble substance with a high deliquescence relative humidity which is present in the atmosphere (Wex et al., 2007), while levoglucosan is an organic substance known to be a tracer for biomass burning (Simoneit et al., 1999) with a much higher solubility.

A sketch of the general set-up can be seen in Fig. 1. To disperse kaolinite particles, a fluidized bed generator (TSI 3400A, TSI Inc., St. Paul, Minnesota, USA) was used. In order to reduce the number of charges carried on the particles, and therewith to reduce the loss of charged particles to walls within the particle generation set-up, a corona discharger was put in line behind the fluidized bed. The corona was produced on top of a needle to which high voltage (4 kV) was applied. We wanted to examine size selected particles, and to facilitate the size selection, a rough pre-selection was done, i.e. particles with aerodynamic diameters above 560 nm or 1000 nm (for the generation of 300 nm or 700 nm particles, respectively) were separated with a MOUDI impactor (Micro Orifice Uniform Deposition Impactor, Model 100R, MSP Corporation, Shoreview, Michigan, USA). Downstream of the MOUDI, a neutralizer established a bipolar equilibrium charge distribution on the particles.

When a coating was applied to the particles, the aerosol was then sent through one of three thermostated glass tubes, which contained either a reservoir filled with succinic acid ($C_4H_6O_4$, SuccA will be used as abbreviation for it from here on), levoglucosan ($C_6H_{10}O_5$, abbreviated LG) or with sulfuric acid (H_2SO_4). The temperature of the tubes was controlled via thermostats (HAAKE C25P, HAAKE GmbH, Karlsruhe, Germany). The glass tubes were set to temperatures between 45 °C and 90 °C, depending on

ACPD
13, 30311–30348, 2013

Kaolinite particles as ice nuclei

H. Wex et al.

the material and the desired coating thickness. For particles coated with H_2SO_4 at 70 °C, a further treatment was sometimes applied, i.e. water vapor was added to the aerosol by sending it over a water bath at room temperature and subsequently sending it through a second diffusion drier (not shown in the sketch).

The coating section could also be bypassed, but whether coated or not, particles were then sent through a DMA (Differential Mobiliy Analyzer, Type Vienna Hauke medium, aerosol to sheath air flow ratio of 1 : 10) to select particles with one mobility. Selected mobility diameters were either 300 nm or 700 nm throughout the experiments described herein. The aerosol was then distributed to the different instruments. In this part of the set-up, two additional flows of particle free air were added, where the particle number concentration was roughly halved in each of the steps. The different flows were controlled frequently, using a bubble flow meter, to enable the calculation of particle concentrations delivered to the different instruments. It was also ensured that a small excess of aerosol was produced. The small excess flow was vented in order to maintain the pressure in the whole particle generation set-up close to laboratory pressure.

Directly downstream of the DMA, the aerosol was fed into LACIS (Leipzig Aerosol Cloud Interaction Simulator), which was used to measure immersion freezing (Hartmann et al., 2011). LACIS consists of a 7 m long flow tube where each 1 m section can be temperature controlled separately. Temperatures can go down to −50 °C. Before entering the flow tube, by use of a humidifier (PH-30T-24KS, Perma Pure), the sheath air stream is hydrated such that droplets form on the aerosol particles upon cooling, i.e. during the passage of the flow tube. These droplets can subsequently freeze, depending on the nature of the immersed aerosol particle and the adjusted temperature. A detailed analysis of thermodynamic profiles in LACIS can be found in Hartmann et al. (2011). At the LACIS outlet, a self built optical particle spectrometer (TOPS-Ice, Clauss et al., 2013) determines if the arriving hydrometeors are liquid droplets or frozen ice crystals, resulting in the determination of a frozen fraction, f_{ice}, i.e., the number of frozen droplets divided by the total number of liquid and frozen droplets.

Particle number concentrations were measured with a Condensation Particle Counter (CPC, TSI 3010), which was operated in parallel to a Cloud Condensation Nucleus counter (CCNc, Droplet Measurement Technologies) to determine the activation of the particles to cloud droplets and from that the coating thicknesses. Using both, data from CPC and CCNc, the fraction of all particles activated was determined. During the measurements, the supersaturation in the CCNc was scanned such that full activation curves, i.e. from none to all particles activated, were obtained.

Ice nucleation was also measured using a CFDC (Continuous Flow Diffusion Chamber, Rogers et al., 2001; DeMott et al., 2010). The particle number concentrations delivered to this instrument were a few tens per cubic centimeter. The CFDC is operated with ice covered walls which are kept at different temperatures. Temperatures can be set such that both, sub- or supersaturation with respect to water vapor can be achieved for a focused aerosol lamina within the instrument. Evaporation of only liquid particles within the last section of the instrument facilitates optical detection of nucleated ice crystals. In this study, the IN number concentrations were determined as a function of water vapor saturation by stepwise scanning experimental conditions from ice saturation to a relative humidity (with respect to liquid water, RH_w) of about 107 %. It is assumed that although all ice formation mechanisms are possible in the regime above 100 % RH_w, this condition favors condensation/immersion freezing nucleation. Particularly close to 100 % RH_w, it might be possible that the particles are not activated to diluted droplets but form haze particles, instead, and the term condensation freezing should be understood correspondingly. To obtain frozen fractions, f_{ice}, from the CFDC measurements, measured total particle number concentrations were used together with the IN number concentrations, i.e. the same parameter was derived that was also obtained from the LACIS measurements.

ACPD
13, 30311–30348, 2013

3 Results and discussion

3.1 Coating thicknesses

We first discuss the amount of coatings present on the examined particles. Besides examining 300 nm particles from either Fluka or CMS kaolinite samples, also 700 nm Fluka kaolinite particles were used. Different coating temperatures were applied for all three coating substances, SuccA, LG and H_2SO_4, where for the latter additionally water vapor was added in some cases. Particle generation was operated such that for the course of one experiment, which usually lasted around 2 h, one type of particle with one type of coating was produced, while the different instruments examined the particles. The need for CFDC and LACIS to either re-ice or defrost, respectively, determined the length of an experiment. Some particle types were generated repeatedly for more than one of these 2 hourly time-spans.

Scans of activated fractions vs. supersaturation were measured with the CCNc for all the different particle types. The critical supersaturations for droplet activation, i.e. the supersaturation at which 50 % of all particles were activated, were derived applying an error function fit to the measured activated fraction curves.

The critical supersaturation for the pure particles were found to be 0.29 % and 0.44 % for the 300 nm Fluka and CMS kaolinite particles, respectively, and 0.17 % for Fluka particles of 700 nm. These critical supersaturations are lower than expected for purely insoluble particles. Still, when using kappa-Köhler theory (Petters and Kreidenweis, 2007), these values correspond to kappa-values below 0.005. Comparable or even larger kappa-values have been reported for different mineral dusts e.g. in Herich et al. (2009) and Koehler et al. (2009), i.e. mineral dust particles generally were observed to be more easily activated to a droplet than expected. Kumar et al. (2011) attributed this fact to adsorption of water on the insoluble component of the dust particle. However, Herich et al. (2009) and Koehler et al. (2009) both also found that the kappa-value of the mineral dust particles increased when the particles had been sprayed from an aqueous solution (instead of dispersing them from a dry powder), and argued that this was due

Discussion Paper | Discussion Paper | Discussion Paper | Discussion Paper |

ACPD
13, 30311–30348, 2013

Kaolinite particles as ice nuclei

H. Wex et al.

to a redistribution of small amounts of soluble material which had to have been present already on the dry particles. We follow that line of argument, i.e. we assume that a small amount of soluble impurities was present on the kaolinite particles examined in this study. Based on the observed critical supersaturations it can be estimated that this amounts to less than 1 % of the mass of the examined particles.

Coated particles activated at lower supersaturations than the pure ones, due to the larger soluble mass available. This decrease in supersaturation between uncoated and coated particles was used to derive the amount of soluble material which had been added to the particle during coating. We assumed that the particles were spherical with an insoluble core and a mantle of soluble material of either SuccA, LG or H_2SO_4 around them, depending on the coating. Derived coating thicknesses are given in Table 1.

It should be mentioned that at least the H_2SO_4 coating most likely will have chemically reacted with the dust particles. Reitz et al. (2011) examined ATD (Arizona Test Dust) particles coated with H_2SO_4, where the coating procedure was similar to the one in the present study, and it was reported that both sulfuric acid as well as sulfates were present on the particles. This suggests a reaction between the H_2SO_4 coating and the ATD. As the derived amount of coating depends on the hygroscopicity of the coating material, and as sulfates commonly have a lower hygroscopicity than sulfuric acid, coating thicknesses derived from our data could be up to a factor of 2 above those given in Table 1 for the H_2SO_4 coatings. Nevertheless, the derived coating thicknesses still can give a rough estimate and should only be viewed as such.

With sizes of the molecules of SuccA, LG and H_2SO_4 roughly in the range of 0.5 nm, and with the shape of the particles likely being rather flaky than spherical, the coatings that were obtained for the lowest coating temperatures can be expected to not cover the whole particle surface, while the highest coating temperatures are much more likely to having produced a complete coating in all cases.

ACPD
13, 30311–30348, 2013

3.2 Immersion freezing

Figure 2 shows exemplary freezing results from both, CFDC and LACIS, for two particle types. Shown are values for f_{ice}, directly inferred from the measurements, and also for j_{het}, the heterogeneous freezing rate coefficient, calculated assuming pure stochastic freezing. The latter was obtained following e.g. Murray et al. (2012):

$$f_{ice} = 1 - \exp(-j_{het} \cdot s \cdot t) \tag{1}$$

with the surface area of the examined particles s and the freezing time t. While t was 1.6 s for the LACIS measurements (see Hartmann et al., 2011), a residence time of 5 s was used for the CFDC, based on the maximum time for immersion freezing (104–106 % RH_w) in the CFDC, following the model of Rogers (1988) (see DeMott et al., 2013).

A stochastic approach for the description of immersion freezing induced by kaolinite has e.g. also been used in Murray et al. (2011), where a single type of active site was sufficient to describe the observed immersion freezing for a suite of different experimental conditions for a CMS kaolinite sample. The likely homogeneity of active sites on kaolinite and the short instrument residence times justify and likely also require the stochastic rate analysis in our study. We may note that in Broadley et al. (2012), a study on illite particles which are considered as a more representative surrogate for atmospheric dusts, the use of a multi-component stochastic model was required or, alternatively, the data could be approximated as freezing deterministically (without time dependence) for the purpose of atmospheric modeling.

Values for f_{ice} given in Fig. 2 were fitted separately for the data from CFDC and from LACIS, and the curves are shown in the upper panels. An apparent shift in the data from CFDC to LACIS of about 2 K could be interpreted from these curves. The fact that an analysis of j_{het} brings the data into better alignment in the lower panel of Fig. 2 is consistent with the assumption of stochastic freezing for kaolinite particles, i.e. with the assumption that freezing is a time dependent process, corroborating the results by Murray et al. (2011).

ACPD
13, 30311–30348, 2013

The two experiments shown in Fig. 2 are similar to what was found for all coated and uncoated kaolinite particles examined in this study. That is, analysis of j_{het} always led to merger of data from CFDC and LACIS. Hence data from the two instruments were combined and fitted as one data-set. This was done using:

$$j_{\text{het}} = A \cdot \exp(B \cdot T) \quad (2)$$

where T is the temperature (expressed in °C), A and B are the fitting parameters. Examples for the resulting fitting curves are included in the two lower panels of Fig. 2. A and B were derived for all particle types for which data from both, the CFDC and LACIS, were available. All resulting fitting curves are displayed in Fig. 3, while resulting values for A and B are shown in Fig. 4.

It has to be added that A and B were derived for the temperature range in which the measurements had been done, indicated by the grey shaded area in Fig. 3, and for residence times on the order of a few seconds. Hence the parameterizations underlying the curves shown for kaolinite IN in Fig. 3 are not necessarily valid outside the grey shaded area, nor for much longer time scales.

The curves displayed in Fig. 3 roughly split into two groups, with the blue curve, i.e. the one for 300 nm Fluka kaolinite particles coated with the thinnest H_2SO_4 coating, applied at only 45 °C, belonging to neither. The first group of curves includes data for pure Fluka kaolinite (green curve) and data for all Fluka kaolinite particles which were pure or coated with either SuccA or LG (curves colored black). Error bars depicting one standard deviation were added exemplarily to the green curve. The red and orange curves were used for the second group, containing all CMS kaolinite particles, regardless of the coating, and additionally also the Fluka kaolinite particles which had been coated with H_2SO_4 at 70 °C (with or without additionally water vapor). Again, the two orange curves have error bars added to them, exemplarily. (It should be pointed out that the lower orange curve almost completely coincides with the next lower red curve, hence only 7 different red or orange curves are clearly visible.) It can be seen that the CMS kaolinite particles and particles coated with H_2SO_4 are generally less ice active than particles belonging to the first group for temperatures above about −34 °C. Among all 300 nm Fluka kaolinite particles coated with H_2SO_4, those with the thinnest coating (blue curve) are clearly still the most ice active, indicating that the respective smaller amount of coating did not destroy the ice nucleation ability as thoroughly as did the thicker coatings.

We will now turn to Fig. 4, which resolves details better than Fig. 3. It can be seen that *A* and *B* show the same tendencies, i.e. when lower values were obtained for *A*, also lower values were obtained for *B*. When results were available for both, 300 nm and 700 nm Fluka kaolinite, they were always similar, as to be expected since the particle size is accounted for when deriving j_{het}.

One of the most noticeable features in Fig. 4 is, that the parameters obtained for the CMS kaolinite particles are clearly lower than those for the Fluka kaolinite for all particles except for those coated with H_2SO_4. This agrees with literature available on immersion freezing of kaolinites, where generally CMS kaolinite was found to be less ice active than the Fluka kaolinite: Murray et al. (2011) used CMS kaolinite in their study and reported that they found a lower ice nucleation ability than Lüönd et al. (2010), a study in which Fluka kaolinite has been used. Pinti et al. (2012) examined CMS kaolinite and kaolinite distributed by Sigma Aldrich (which is the same as that provided by Fluka) and found the Sigma Aldrich kaolinite to be more ice active. We will return to discussing the differences in the two types of kaolinite later in this section.

Coatings of SuccA or LG for all examined coating temperatures had no remarkable influence on the immersion freezing, i.e. *A* and *B* derived for the particles coated with SuccA or LG are similar to those for the respective uncoated particles. This holds true for Fluka and CMS kaolinite particles. This is not surprising, as SuccA and LG are both soluble substances, and for immersion freezing the droplets generated in the CFDC and in LACIS, had maximum sizes above 2 µm (Hartmann et al., 2011; DeMott et al., 2013), i.e. the soluble material on the particles was strongly diluted and freezing point depression is negligible. These results also suggest that SuccA and LG did not alter the surface of the particles chemically.

ACPD
13, 30311–30348, 2013

Concerning coatings of H_2SO_4, the data as shown in Fig. 4 reiterates and expands the point that this type of coating reduces the immersion freezing ability of Fluka kaolinite particles, visible in the lower A and B values. The addition of water vapor was intended to intensify the reaction between the acid and the kaolinite, as it had been observed previously for Arizona Test Dust (ATD, Niedermeier et al., 2011), but this was not observed, here.

Differently than for the Fluka kaolinite, a considerable decrease in the immersion freezing ability due to H_2SO_4 coating was not observed for the CMS kaolinite particles. A data-set sufficient for evaluation exists only for the CMS kaolinite particles coated at 70 °C with additional water vapor, which, however, should have been the most reactive coating produced.

The group of Fluka kaolinite particles of both sizes, either uncoated or coated with SuccA or LG, shows average values of $A_{\text{Fluka}} = 155.4\,\text{m}^{-2}\,\text{s}^{-1}$ and $B_{\text{Fluka}} = -0.57\,°\text{C}^{-1}$. The second group including all CMS kaolinite particles, regardless of the coating, and the Fluka kaolinite particles which had been coated with H_2SO_4 at 70 °C, with or without added water vapor have average values of $A_{\text{CMS}} = 1.21 \times 10^{-5}\,\text{m}^{-2}\,\text{s}^{-1}$ and $B_{\text{CMS}} = -1.03\,°\text{C}^{-1}$.

The grouping of the data shows that although we used a strong acid we were not able to destroy ice nucleation sites on the CMS kaolinite much, however, we were able to do so on the Fluka kaolinite. It can be assumed that the H_2SO_4 coating causes a chemical reaction which alters the Fluka kaolinite, making the remaining particles similar in their IN ability to CMS kaolinite.

These results can be further interpreted when considering a recent publication by Atkinson et al. (2013). In that study, potassium feldspar is considered to be the most efficient ice nucleating dust globally. Atkinson et al. (2013) give the amount of potassium feldspar present in Fluka kaolinite to be roughly 5 %, while CMS kaolinite is reported to not contain any detectable amount. In general, common clay minerals are the weathering product of feldspar (Blum, 1994), and one transformation occurring in the field is the reaction of e.g. potassium feldspar with H^+ and H_2O to form quartz and kaolinite.

Therefore, the different fractions of feldspar in the two examined kaolinite samples hint towards the fact that the Fluka kaolinite is not weathered quite as thoroughly as the CMS kaolinite. The additional natural weathering likely is the reason for the reduced IN ability of the CMS kaolinite particles. The above presented results on immersion freezing of the two different kaolinites hint towards a corroboration of the claim by Atkinson et al. (2013), i.e. that it might indeed be the potassium feldspar which is responsible for an increased IN ability in some dusts.

3.3 Ice nucleation under water subsaturated conditions

Now we will introduce measurements of ice nucleation in the regime below water saturation where deposition nucleation or freezing of haze particles may occur. These measurements were done only with the CFDC. Figure 5 shows f_{ice} as determined with the CFDC for 300 nm Fluka, 300 nm CMS and 700 nm Fluka kaolinite particles for water subsaturated conditions, for pure particles and those with medium thick and thick coatings. Measurements for Fluka kaolinite were done at −26 °C, −30 °C and −34 °C, while the CMS kaolinite measurements were made at −30 °C, −34 °C and −38 °C. Compared to Fluka kaolinite particles, the CMS kaolinite particles were less active for ice nucleation in the water subsaturated regime, similar to what was observed for immersion freezing of particles in dilute solutions above water saturation.

Results for 300 nm Fluka, 300 nm CMS and 700 nm Fluka kaolinite share some features in the observed ice nucleation in the water subsaturated regime: (1) the uncoated kaolinite particles showed ice nucleation at a water vapor saturation ratio (S_w) below 0.95 clearly occurring at temperatures below −34 °C and even already at −30 °C for the 700 nm Fluka kaolinite particles. (2) The coated particles examined here, which all had coating thicknesses above 0.5 nm, lost the ability to induce apparent deposition ice nucleation at S_w below 0.95. (3) These particles all started to induce ice at S_w above 0.95, with a steep increase in the measured ice fractions towards saturation. The following paragraphs will show that for these particles with coating thicknesses above 0.5 nm deposition ice nucleation likely can not take place any more, but that instead the measurements follow quantitatively what can be expected when immersion freezing in a concentrated solution takes place.

It is known that soluble material in a solution lowers the ice melting temperature of that solution (ΔT_m) compared to pure water, and that this lowering depends on the concentration, i.e. on the water activity (a_w), of the solution. This lowering is reflected in a lowering of the homogeneous freezing temperature (ΔT_{hom}). It was observed that there is a proportional relationship between ΔT_{hom} and ΔT_m, yielding the so called λ-approach: $\Delta T_{hom} = \lambda_{hom} \Delta T_m$. This approach has first been described by MacKenzie et al. (1977) and Rasmussen (1982) and was applied to model atmospheric homogenous freezing of droplets as early as in Sassen and Dodd (1988). Following Koop and Zobrist (2009) and literature citetd therein, λ_{hom} can be expected to be on the order of 2 to 2.5 for the soluble substances we examined in our study.

The λ-approach can be extended to solutions with immersed IN, as suggested already in DeMott (2002) and applied e.g. in Zuberi et al. (2002), Archuleta et al. (2005) and Koop and Zobrist (2009) (where the latter gives an overview of publications on this topic). The extended λ-approach results in a relationship between ΔT_m and the freezing point depression for heterogeneous freezing (ΔT_{het}): $\Delta T_{het} = \lambda_{het} \Delta T_m$, where generally $1 < \lambda_{het} < \lambda_{hom}$.

For our study, values for ΔT_m vs. a_w were taken from Koop and Zobrist (2009). For the CFDC data, Köhler theory was used to convert S_w as adjusted during the measurements to a_w. For a coated kaolinite particle exposed to water vapor, the soluble material on the particle will dissolve as soon as S_w in the surroundings is above the deliquescence point of the soluble material, and (providing equilibrium is reached) a solution with a_w close to S_w will then be present on the particle surface. For a_w of e.g. 0.95 (where $\Delta T_m = 5.3$, Koop and Zobrist, 2009), the respective solution will cause a ΔT_{het} of 10.6 K or 13.3 K for a λ_{het} of 2 or 2.5, respectively. Figure 6 illustrates what follows from this: the ice nucleation rates and likewise j_{het} need to be shifted to lower temperatures. j_{het} can be calculated based on Eq. (2), using the values of A and B as given in Fig. 4 and assuming that the ice nucleation takes place at a temperature which is increased

Discussion Paper | Discussion Paper | Discussion Paper | Discussion Paper |
ACPD
13, 30311–30348, 2013
Kaolinite particles as ice nuclei
H. Wex et al.

by ΔT_{het} compared to the temperature of the surrounding. This causes j_{het} to be shifted in the direction of the arrow in Fig. 6. The black curve shows j_{het} for uncoated 300 nm Fluka kaolinite particles, based on the respective A and B given in Fig. 4. The curves in different shades of grey show this same curve for such particles immersed in solutions with $0.99 \leq a_w \leq 0.94$ for a λ_{het} of 2. The black vertical line indicates which values for j_{het} would be expected at −34 °C for differently concentrated solutions, showing that e.g. at an a_w of 0.95, j_{het} is reduced by roughly three orders of magnitude.

For our further analysis, a combination of Eqs. (1) and (2), including the freezing point depression, was used:

$$f_{ice}(a_w) = 1 - \exp(-A \cdot \exp(B \cdot (T + \Delta T_{het}(a_w)))s \cdot t) \quad (3)$$

The average values A_{Fluka} and B_{Fluka} were used, together with the residence time in the CFDC of 5 s, to calculate f_{ice} at −34 °C for the 300 nm and 700 nm Fluka kaolinite particles, as a function of water activity. Results are shown in Fig. 7 as grey shaded areas, which cover results for λ_{het} between 1 (left edge) and 2.5 (right edge) and which show a grey line in their middle for $\lambda_{het} = 1.7$. λ_{het} of 1 and 2.5 are a conservative lower and upper bound, where for $\lambda_{het} = 1$ it would be $\Delta T_{het} = \Delta T_{hom} = \Delta T_m$, and therefore this bound can be expected to underestimate the freezing point depression and likewise the suppression of freezing. A λ_{het} of 1.7 was chosen as this value was found in Zuberi et al. (2002) to fit their data for freezing of kaolinite and montmorillonite particles in aqueous solutions containing $(NH_4)_2SO_4$. Also shown in Fig. 7 is f_{ice} measured with the CFDC for medium and thickly coated particles.

These grey shaded areas now represent the range where freezing induced by the pure particles can be expected, when they are immersed in a solution. And indeed, both the observed temperature range and slope of the measured freezing behavior for the Fluka kaolinite particles coated with SuccA and LG are well captured. It should be noted here that the CFDC has an uncertainty in relative humidity of roughly 3 %, i.e. about 0.03 in water activity, so that measured and calculated values all agree within uncertainty.

It has to be noted here explicitly, that the parameters A_{Fluka} and B_{Fluka} determined from the immersion freezing are valid for the Fluka kaolinite in our experiments as long as it is not coated with H_2SO_4, i.e. as long as it is not altered. Applying the above described model to Fluka kaolinite coated with H_2SO_4 or to CMS kaolinite requires use of the average values of A_{CMS} and B_{CMS}. When this is done, the redly striped areas in Fig. 7 are obtained. Again, a grey line represents results for $\lambda_{\mathrm{het}} = 1.7$. For the Fluka kaolinite particles, the location of the redly striped areas, compared to the grey areas, reflect the fact that these particles showed a reduced immersion freezing ability upon coating with H_2SO_4, hence they are shifted to lower f_{ice} (or seemingly larger water activities). For CMS kaolinite, only the redly striped area is shown, as these particles did not show a change in the immersion freezing upon any of the coatings.

When comparing the measured values for the two different groups of IN, indeed, the 300 nm Fluka kaolinite particles coated with either SuccA or LG show an increased freezing ability compared to these particles coated with H_2SO_4 (with or without additional water vapor). Such a clear difference in f_{ice} between SuccA and LG coating to the two coatings with H_2SO_4 is not seen for the 300 nm CMS kaolinite particles, where it would not have been expected. All in all, when considering the above mentioned measurement uncertainty of the CFDC and including all particles and coatings, measured and calculated values are well in agreement within uncertainty in the examined λ_{het} range and even with λ_{het} of 1.7. Unfortunately, the measurement uncertainties do not allow for a more constrained determination of λ_{het}.

Our results support that particles with medium thick and thick coatings examined in our study did not show deposition ice nucleation behavior any more, in the whole range of $S_w < 1$. At relative humidities below the deliquescence point of the coating material, ice nucleation sites were covered and freezing was inhibited. Above the deliquescence relative humidity, additional water was added to the coating and a solution shell formed around the particles, causing them to rather nucleate ice from concentrated solutions via the immersion freezing pathway. The solutions were so concentrated that immersion freezing was quenched due to freezing point depression. This is well in line with observations reported in Archuleta et al. (2005), Eastwood et al. (2009) and Sullivan et al. (2010a), where it was concluded for the heterogenous freezing of coated particles in the water vapor subsaturated range that freezing could only be initiated once the coating was dissolved.

An open issue is, why also SuccA, a slightly soluble substance, seems to form a solution at water activities below 0.99, where it should not dissolve. However, as stated above, likely the applied coatings were not the only soluble materials on the particle surfaces. Mixtures tend to deliquescence at lower S_w than the pure substances (Marcolli et al., 2004), and the co-existence of the coating material with impurities on the kaolinite surfaces might be an explanation for the observations.

Figure 8 shows the relation of S_w to the water vapor saturation ratio above ice (S_i) as function of temperature, in a way which is typical for displaying results particularly for deposition ice nucleation. A black, grey and light grey line correspond to S_w of 1, 0.9 and 0.8, respectively. For reference, a dash-dotted line is shown for homogeneous freezing of solution droplets taken from Koop et al. (2000). Furthermore, lines are inserted which are based on the above presented parameterization (Eq. 3) for 300 nm and 700 nm Fluka kaolinite particles with LG or SuccA coatings, assuming a λ_{het} of 1.7. The lines correspond to a frozen fraction (f_{ice}) of 0.1 % and 1 %. These lines and the one for $S_w = 1$ limit the range in which the above described effect, i.e. immersion freezing of concentrated solution droplets, can occur in our study. This range will become larger for larger nucleation rates ($j_{het} \cdot s$), i.e. either for larger particles (as can e.g. be seen by comparing the data for 300 nm and 700 nm in Fig. 8), or for more ice active IN (e.g biological IN, see Murray et al., 2012). Deposition ice nucleation can still occur within this range when a potential IN is not completely coated. However, in literature the range of freezing onsets (temperature and S_w) reported for deposition ice nucleation is very large for any one IN particle type (Hoose and Möhler, 2012), and besides instrumental and experimental issues some of this scatter might be explained by wrongly attributing immersion freezing in concentrated solutions to deposition ice nucleation instead.

ACPD
13, 30311–30348, 2013

The above described results support the hypothesis that condensation and immersion freezing (i.e. the ice nucleation of an insoluble core immersed in a haze particle or in a diluted droplet) might basically be the same process, with the only distinction that a freezing point depression has to be accounted for in the subsaturated regime (i.e. for the haze particles). Equation (3) (and likely also other temperature dependent parameterizations) could be used to describe both, the freezing of droplets consisting of concentrated or dilute solutions with an immersed ice nucleus, where only care has to be taken to include the freezing point depression for the concentrated solutions correctly, whereas $\Delta T_{\text{het}} = 0$ for diluted solutions. In e.g. Khvorostyanov and Curry (2004) it is argued that atmospheric IN are not necessarily insoluble but that rather a significant fraction is mixed with soluble material, motivating the development of a model describing "deliquescent-heterogenous freezing" following a concept comparable to the one we used here. It is not a new idea when we argue that condensation and immersion freezing are similar, but by including a comparison of measured and modeled data for both, the sub- and supersaturated regime, we corroborated this assumption. Future work should aim at testing our hypothesis, making maybe a discrimination between the two modes, condensation and immersion freezing, unnecessary.

4 Summary and conclusions

In the present study, we examined immersion freezing and ice nucleation in the water subsaturated regime for size segregated particles from two types of kaolinite, provided by Fluka and CMS. Pure particles were examined, and also particles with coatings of below up to a few nanometers of sulfuric acid (H_2SO_4), succinic acid (SuccA) and levoglucosan (LG). Freezing measurements were done using two different instruments, LACIS (Hartmann et al., 2011) and a CFDC (DeMott et al., 2010), where both instruments measured in the water supersaturated regime, while deposition ice nucleation or other mechanisms possible in the water subsaturated regime were only examined by the CFDC.

ACPD
13, 30311–30348, 2013

Frozen fractions observed by the two instruments in the immersion freezing regime differed. However, when considering a time dependence of the freezing process based on a single component stochastic approach, i.e. when comparing nucleation rate coefficients, these differences vanished, i.e. the data observed by LACIS and the CFDC were in agreement. We should note that the approach which we used may not be a general result for all types of IN. For example, in Broadley et al. (2012) heterogenous freezing induced by NX-illite particles could not be characterized by a single component stochastic model but instead by either a multi component stochastic model or a deterministic model. Also, DeMott et al. (2013) discuss other instrumental factors for the CFDC that require clarification before all caveats may be removed in interpreting data from this instrument stochastically.

Our results concerning the IN ability of the pure minerals corroborate earlier findings, i.e. CMS kaolinite generally was found to be less ice active than Fluka kaolinite in both, immersion freezing and in deposition ice nucleation, and deposition ice nucleation generally was found to be the less effective heterogenous freezing process, compared to immersion freezing.

In case of immersion freezing, the organic coatings used in our study did not reduce the IN ability of either kaolinite, i.e. these coatings did not alter the surface of the particles irreversibly and formed a very dilute solution when the particles were activated to droplets prior to freezing. On the other hand, H_2SO_4 coatings did reduce the IN ability of the Fluka kaolinite remarkably, but left the IN ability of the CMS kaolinite almost unchanged. This observation could potentially be explained by attributing the higher IN ability of the Fluka kaolinite to its content of potassium feldspar, a mineral which is not present in the CMS kaolinite and which likely is destroyed on contact with H_2SO_4. This hypothesis aligns with a recent publication by Atkinson et al. (2013), where potassium feldspar is assumed to be the most important mineral dust for atmospheric ice nucleation.

Ice nucleation at below water saturation was found to be impeded by all coatings with coating thicknesses above 0.5 nm for S_w below about 0.95, while at $S_w \geq 0.95$

a steep increase in the observed freezing was seen. Consistent with previous hypotheses, we showed that these observations can be explained by assuming that deposition ice nucleation likely does not take place any more for the examined particles, but that instead the measurements follow what can be expected when immersion freezing in a concentrated solution takes place. The coatings examined in this case correspond to a hygroscopicity parameter kappa of the overall dust particle of about 0.05, showing that the amount of soluble material present on a particle which suffices to hinder deposition ice nucleation is small. This might explain some of the observed scatter in the data for deposition ice nucleation reported in literature in the past, i.e. some of the observation might not have been deposition ice nucleation but immersion freezing in a concentrated solution, instead. This also points towards the possibility that deposition ice nucleation might play an even smaller role in atmospheric processes than so far expected.

The fact that the parameterization we derived for the immersion freezing regime could also be used to model the freezing behavior of the IN immersed in concentrated solution droplets indicates that maybe all freezing processes which include a (more or less concentrated) solution shell which formed around an IN prior to freezing might be treated as being the very same process. The term immersion freezing has generally been used for all cases when an insoluble particle is immersed in a diluted droplet. Although the definition of condensation freezing has previously been less well defined, we argue that this should include all cases when an insoluble particle is immersed in a concentrated solution (i.e. in the case of haze particles), which principally can occur for $S_w < 1$ as long as the deliquescence RH of the soluble material which was on the insoluble core prior to forming a solution is overcome. We show in the present study, that these two heterogenous freezing modes, i.e. condensation and immersion freezing, can be treated similarly, only by accounting for a freezing point depression for the haze particles. This potentially reduces the number of heterogenous freezing processes which need to be considered separately in atmospheric models to three,

ACPD
13, 30311–30348, 2013

namely deposition ice nucleation, contact freezing and the here examined condensation/immersion freezing.

Acknowledgements. Financial support for this study was obtained from the German Science Foundation within the framework of the Ice Nucleation research UNiT (DFG Research Unit FOR 1525 INUIT, grant WE 4722/1-1). PJD and YT acknowledge partial support from US NSF grant ATM-0841602 and the EUROCHAMP II program. YT also acknowledges the JSPS Postdoctoral Fellowships for Research Abroad.

References

Ansmann, A., Tesche, M., Seifert, P., Althausen, D., Engelmann, R., Fruntke, J., Wandinger, U., Mattis, I., and Müller, D.: Evolution of the ice phase in tropical altocumulus: samum lidar observations over Cape verde, J. Geophys. Res., 114, D17208, doi:10.1029/2008JD011659, 2009. 30313

Archuleta, C. M., DeMott, P. J., and Kreidenweis, S. M.: Ice nucleation by surrogates for atmospheric mineral dust and mineral dust/sulfate particles at cirrus temperatures, Atmos. Chem. Phys., 5, 2617–2634, doi:10.5194/acp-5-2617-2005, 2005. 30314, 30315, 30327, 30330

Atkinson, J. D., Murray, B. J., Woodhouse, M. T., Whale, T. F., Baustian, K. J., Carslaw, K. S., Dobbie, S., O'Sullivan, D., and Malkin, T. L.: The importance of feldspar for ice nucleation by mineral dust in mixed-phase clouds, Nature, 498, 355–358, 2013. 30314, 30315, 30317, 30325, 30326, 30332

Blum, A. E.: Feldspars in Weathering, Feldspars and Their Reactions, Springer, the Netherlands, 1994. 30325

Broadley, S. L., Murray, B. J., Herbert, R. J., Atkinson, J. D., Dobbie, S., Malkin, T. L., Condliffe, E., and Neve, L.: Immersion mode heterogeneous ice nucleation by an illite rich powder representative of atmospheric mineral dust, Atmos. Chem. Phys., 12, 287–307, doi:10.5194/acp-12-287-2012, 2012. 30322, 30332

Burrows, S. M., Hoose, C., Pöschl, U., and Lawrence, M. G.: Ice nuclei in marine air: biogenic particles or dust?, Atmos. Chem. Phys., 13, 245–267, doi:10.5194/acp-13-245-2013, 2013. 30314

Clauss, T., Kiselev, A., Hartmann, S., Augustin, S., Pfeifer, S., Niedermeier, D., Wex, H., and Stratmann, F.: Application of linear polarized light for the discrimination of frozen and liquid

ACPD
13, 30311–30348, 2013

droplets in ice nucleation experiments, Atmos. Meas. Tech., 6, 1041–1052, doi:10.5194/amt-6-1041-2013, 2013. 30318

Cziczo, D. J., Murphy, D. M., Hudson, P. K., and Thomson, D. S.: Single particle measurements of the chemical composition of cirrus ice residue during crystal-face, J. Geophys. Res., 109, D04201, doi:10.1029/2003JD004032, 2004. 30314

Cziczo, D. J., Froyd, K. D., Gallavardin, S. J., Moehler, O., Benz, S., Saathoff, H., and Murphy, D. M.: Deactivation of ice nuclei due to atmospherically relevant surface coatings, Environ. Res. Lett., 4, 044013, doi:10.1088/1748-9326/4/4/044013, 2009. 30315

Cziczo, D. J., Froyd, K. D., Hoose, C., Jensen, E. J., Diao, M., Zondlo, M. A., Smith, J. B., Twohy, C. H., and Murphy, D. M.: Clarifying the dominant sources and mechanisms of cirrus cloud formation, Science, 340, 1320–1324, 2013. 30313

de Boer, G., Morrison, H., Shupe, M. D., and Hildner, R.: Evidence of liquid dependent ice nucleation in high-latitude stratiform clouds from surface remote sensors, Geophys. Res. Lett., 38, L01803, doi:10.1029/2010GL046016, 2011. 30313

DeMott, P. J.: Laboratory studies of cirrus cloud processes, in Cirrus, edited by: Lynch, D. K., Sassen, K., Starr, D. O. C., and Stephens, G., Oxford University Press, 102–135, 2002. 30327

DeMott, P., Sassen, K., Poellot, M. R., Baumgardner, D., Rogers, D. C., Brooks, S. D., Prenni, A. J., and Kreidenweis, S. M.: African dust aerosols as atmospheric ice nuclei, Geophys. Res. Lett., 30, 1732, doi:10.1029/2003GL017410, 2003. 30314

DeMott, P. J., Prenni, A. J., Liu, X., Kreidenweis, S. M., Petters, M. D., Twohy, C. H., Richardson, M. S., Eidhammer, T., and Rogers, D. C.: Predicting global atmospheric ice nuclei distributions and their impact on climate, P. Natl. Acad. Sci. USA, 107, 11217–11222, 2010. 30316, 30319, 30331

DeMott, P. J., Prenni, A. J., McMeeking, G. R., Sullivan, R. C., Petters, M. D., Tobo, Y., McCluskey, C. S., Niemand, M., Möhler, O., Snider, J. R., Sevier, G., and Kreidenweis, S. M.: A parameterization of freezing nucleation by mineral dust particles, in preparation, 2013. 30322, 30324, 30332

Eastwood, M. L., Cremel, S., Wheeler, M. Murray, B. J., Girard, E., and Bertram, A. K.: Effects of sulfuric acid and ammonium sulfate coatings on the ice nucleation properties of kaolinite particles, Geophys. Res. Lett., 36, L02811, doi:10.1029/2008GL035997, 2009. 30315, 30330

ACPD
13, 30311–30348, 2013

Kaolinite particles as ice nuclei

H. Wex et al.

Hallett, J. and Mossop, S. C.: Production of secondary ice particles during the riming process, Nature, 249, 26–28, 1974. 30313

Hartmann, S., Niedermeier, D., Voigtländer, J., Clauss, T., Shaw, R. A., Wex, H., Kiselev, A., and Stratmann, F.: Homogeneous and heterogeneous ice nucleation at LACIS: operating principle and theoretical studies, Atmos. Chem. Phys., 11, 1753–1767, doi:10.5194/acp-11-1753-2011, 2011. 30316, 30318, 30322, 30324, 30331

Herich, H., Tritscher, T., Wiacek, A., Gysel, M., Weingartner, E., Lohmann, U., Baltensperger, U., and Cziczo, D. J.: Water uptake of clay and desert dust aerosol particles at sub- and supersaturated water vapor conditions, Phys. Chem. Chem. Phys., 11, 7804–7809, 2009. 30320

Hoffmann, N., Duft, D., Kiselev, A., and Leisner, T.: Contact freezing efficiency of mineral dust aerosols studied in an electrodynamic balance: quantitative size and temperature dependence for illite particles, Faraday Discuss., doi:10.1039/C3FD00033H, 2013. 30314

Hoose, C. and Möhler, O.: Heterogeneous ice nucleation on atmospheric aerosols: a review of results from laboratory experiments, Atmos. Chem. Phys., 12, 9817–9854, doi:10.5194/acp-12-9817-2012, 2012. 30314, 30315, 30330

Kanji, Z. A., Florea, O., and Abbatt, J. P. D.: Ice formation via deposition nucleation on mineral dust and organics: dependence of onset relative humidity on total particulate surface area, Environ. Res. Lett., 3, 025004, doi:10.1088/1748-9326/3/2/025004, 2008. 30314

Khvorostyanov, V. I. and Curry, J. A.: The theory of ice nucleation by heterogeneous freezing of deliquescent mixed CCN, Part I: Critical radius, energy, and nucleation rate, J. Atmos. Sci., 61, 2676–2691, 2004. 30314, 30331

Koehler, K. A., Kreidenweis, S. M., DeMott, P. J., Petters, M. D., Prenni, A. J., and Carrico, C. M.: Hygroscopicity and cloud droplet activation of mineral dust aerosol, Geophys. Res. Lett., 36, L08805, doi:10.1029/2009GL037348, 2009. 30320

Koop, T. and Zobrist, B.: Parameterizations for ice nucleation in biological and atmospheric systems, Phys. Chem. Chem. Phys., 11, 10839–10850, 2009. 30315, 30327

Koop, T., Luo, B., Tsias, A., and Peter, T.: Water activity as the determinant for homogeneous ice nucleation in aqueous solutions, Nature, 406, 611–614, 2000. 30330, 30348

Kumar, P., Sokolik, I. N., and Nenes, A.: Measurements of cloud condensation nuclei activity and droplet activation kinetics of fresh unprocessed regional dust samples and minerals, Atmos. Chem. Phys., 11, 3527–3541, doi:10.5194/acp-11-3527-2011, 2011. 30320

Lüönd, F., Stetzer, O., Welti, A., and Lohmann, U.: Experimental study on the ice nucleation ability of size-selected kaolinite particles in the immersion mode, J. Geophys. Res., 115, D14201, doi:10.1029/2009JD012959, 2010. 30324

MacKenzie, A. P., Derbyshire, W., and Reid, D. S.: Non-equilibrium freezing behavior of aqueous systems, Philos. T. Roy. Soc. Lond. B, 278, 167–189, 1977. 30327

Marcolli, C.: Deposition nucleation viewed as homogeneous or immersion freezing in pores and cavities, Atmos. Chem. Phys. Discuss., 13, 16367–16456, doi:10.5194/acpd-13-16367-2013, 2013. 30315

Marcolli, C., Luo, B., and Peter, T.: Mixing of the organic fraction: liquids as the thermodynamic stable phases, J. Phys. Chem. A, 108, 2216–2224, 2004. 30330

Murray, B. J., Broadley, S. L., Wilson, T. W., Atkinson, J. D., and Wills, R. H.: Heterogeneous freezing of water droplets containing kaolinite particles, Atmos. Chem. Phys., 11, 4191–4207, doi:10.5194/acp-11-4191-2011, 2011. 30322, 30324

Murray, B. J., O'Sullivan, D., Atkinson, J. D., and Webb, M. E.: Ice nucleation by particles immersed in supercooled cloud droplets, Chem. Soc. Rev., 41, 6519–6554, 2012. 30313, 30314, 30317, 30322, 30330

Niedermeier, D., Hartmann, S., Shaw, R. A., Covert, D., Mentel, T. F., Schneider, J., Poulain, L., Reitz, P., Spindler, C., Clauss, T., Kiselev, A., Hallbauer, E., Wex, H., Mildenberger, K., and Stratmann, F.: Heterogeneous freezing of droplets with immersed mineral dust particles – measurements and parameterization, Atmos. Chem. Phys., 10, 3601–3614, doi:10.5194/acp-10-3601-2010, 2010. 30315

Niedermeier, D., Hartmann, S., Clauss, T., Wex, H., Kiselev, A., Sullivan, R. C., DeMott, P. J., Petters, M. D., Reitz, P., Schneider, J., Mikhailov, E., Sierau, B., Stetzer, O., Reimann, B., Bundke, U., Shaw, R. A., Buchholz, A., Mentel, T. F., and Stratmann, F.: Experimental study of the role of physicochemical surface processing on the IN ability of mineral dust particles, Atmos. Chem. Phys., 11, 11131–11144, doi:10.5194/acp-11-11131-2011, 2011. 30314, 30315, 30325

Petters, M. D. and Kreidenweis, S. M.: A single parameter representation of hygroscopic growth and cloud condensation nucleus activity, Atmos. Chem. Phys., 7, 1961–1971, doi:10.5194/acp-7-1961-2007, 2007. 30320

Pinti, V., Marcolli, C., Zobrist, B., Hoyle, C. R., and Peter, T.: Ice nucleation efficiency of clay minerals in the immersion mode, Atmos. Chem. Phys., 12, 5859–5878, doi:10.5194/acp-12-5859-2012, 2012. 30324

Pruppacher, H. R. and Klett, J. D.: Microphysics of Clouds and Precipitation, Kluwer Academic Publishers, Dordrecht, the Netherlands, 1997. 30314

Rasmussen, D. H.: Thermodynamics and nucleation phenomena – a set of experimental-observations, J. Crystal Growth, 56, 56–66, 1982. 30327

Reitz, P., Spindler, C., Mentel, T. F., Poulain, L., Wex, H., Mildenberger, K., Niedermeier, D., Hartmann, S., Clauss, T., Stratmann, F., Sullivan, R. C., DeMott, P. J., Petters, M. D., Sierau, B., and Schneider, J.: Surface modification of mineral dust particles by sulphuric acid processing: implications for ice nucleation abilities, Atmos. Chem. Phys., 11, 7839–7858, doi:10.5194/acp-11-7839-2011, 2011. 30321

Rogers, D. C.: Development of a continuous flow thermal gradient diffusion chamber for ice nucleation studies, Atmos. Res., 22, 149–181, 1988. 30322

Rogers, D. C., DeMott, P. J., Kreidenweis, S. M., and Chen, Y.: A continous-flow diffusion chamber for airborne measurements of ice nuclei, J. Atmos. Ocean. Tech., 18, 725–741, 2001. 30316, 30319

Sassen, K. and Dodd, G. C.: Homogeneous nucleation rate for highly supercooled cirrus cloud droplets, J. Atmos. Sci., 45, 1357–1369, 1988. 30327

Sassen, K., DeMott, P. J., Prospero, J. M., and Poellot, M. R.: Saharan dust storms and indirect aerosol effects on clouds: crystal-face results, Geophys. Res. Lett., 30, 1633, doi:10.1029/2003GL017371, 2003. 30314

Simoneit, B. R. T., Schauer, J. J., Nolte, C. G., Oros, D. R., Elias, V. O., Fraser, M. P., Rogge, W. F., and Cass, G. R.: Levoglucosan, a tracer for cellulose in biomass burning and atmospheric particles, Atmos. Environ., 33, 173–182, 1999. 30317

Spichtinger, P. and Cziczo, D. J.: Impact of heterogenous ice nuclei on homogenous freezing events in cirrus clouds, J. Geophys. Res., 115, D14208, doi:10.1029/2009JD012168, 2010. 30313

Sullivan, R. C., Minambres, L., DeMott, P. J., Prenni, A. J., Carrico, C. M., Levin, E. J. T., and Kreidenweis, S. M.: Chemical processing does not always impair heterogeneous ice nucleation of mineral dust particles, Geophys. Res. Lett., 37, L24805, doi:10.1029/2010GL045540, 2010a. 30314, 30315, 30316, 30330

Sullivan, R. C., Petters, M. D., DeMott, P. J., Kreidenweis, S. M., Wex, H., Niedermeier, D., Hartmann, S., Clauss, T., Stratmann, F., Reitz, P., Schneider, J., and Sierau, B.: Irreversible loss of ice nucleation active sites in mineral dust particles caused by sulphuric acid condensation, Atmos. Chem. Phys., 10, 11471–11487, doi:10.5194/acp-10-11471-2010, 2010b. 30315

Tobo, Y., DeMott, P. J., Raddatz, M., Niedermeier, D., Hartmann, S., Kreidenweis, S. M., Stratmann, F., and Wex, H.: Impacts of chemical reactivity on ice nucleation of kaolinite particles: a case study of levoglucosan and sulfuric acid, Geophys. Res. Lett., 39, L19803, doi:10.1029/2012GL053007, 2012. 30315, 30316

Vali, G.: Nucleation terminology, J. Atmos. Sci., 16, 575–576, 1985. 30314

Vonnegut, B.: The nucleation of ice formation by silver iodide, J. Appl. Phys., 18, 593–595, 1947. 30313

Welti, A., Lüönd, F., Stetzer, O., and Lohmann, U.: Influence of particle size on the ice nucleating ability of mineral dusts, Atmos. Chem. Phys., 9, 6705–6715, doi:10.5194/acp-9-6705-2009, 2009. 30314

Wex, H., Ziese, M., Kiselev, A., Henning, S., and Stratmann, F.: Deliquescence and hygroscopic growth of succinic acid particles measured with LACIS, Geophys. Res. Lett., 34, L17810, doi:10.1029/2007GL030185, 2007. 30317

Wiacek, A., Peter, T., and Lohmann, U.: The potential influence of Asian and African mineral dust on ice, mixed-phase and liquid water clouds, Atmos. Chem. Phys., 10, 8649–8667, doi:10.5194/acp-10-8649-2010, 2010. 30313

Zimmermann, F., Weinbruch, S., Schütz, L., Hofmann, H., Ebert, M., Kandler, K., and Worringen, A.: Ice nucleation properties of the most abundant mineral dust phases, J. Geophys. Res., 113, D23204, doi:10.1029/2008JD010655, 2008. 30314

Zuberi, B., Bertram, A. K., Cassa, C. A., Molina, L. T., and Molina, M. J.: Heterogeneous nucleation of ice in $(NH_4)_2SO_4$-H_2O particles with mineral dust immersions, Geophys. Res. Lett., 29, doi:10.1029/2001GL014289, 2002. 30315, 30327, 30328

Table 1. Effective coating thicknesses, derived assuming spherical particles with a homogeneous coating.

type of coating	Fluka-kaolinite, 300 nm coating thickness [nm]	CMS-kaolinite, 300 nm coating thickness [nm]	Fluka-kaolinite, 700 nm coating thickness [nm]
H_2SO_4			
45 °C	0.44		
70 °C	1.32	0.87	0.87
70 °C + H_2O	1.77	1.48	1.57
LG			
60 °C	0.20		
80 °C	1.36		
93 °C	3.27	1.85	1.22
SuccA			
70 °C	0.11		
80 °C	0.54		
93 °C	4.78	3.17	1.58

ACPD
13, 30311–30348, 2013

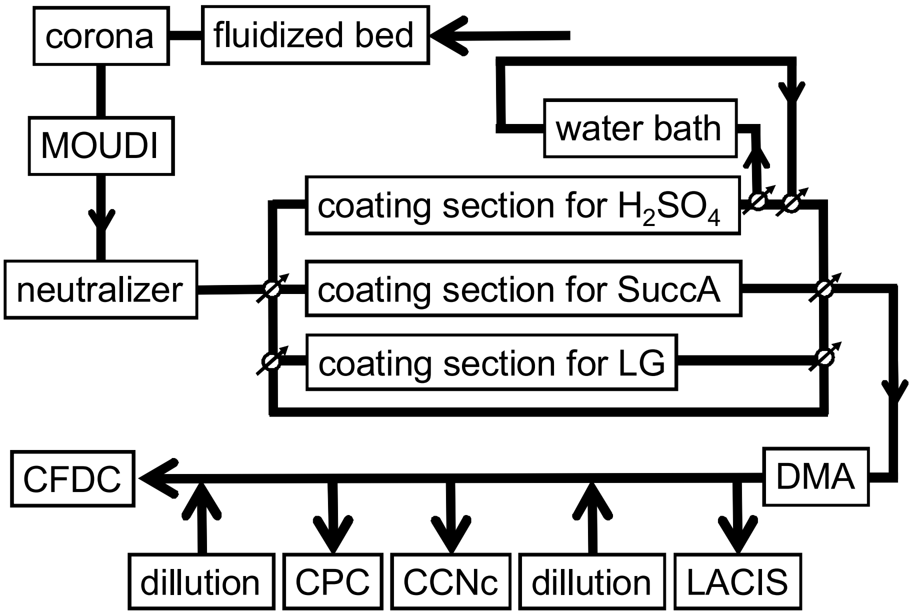

Fig. 1. Set-up of the particle generation.

ACPD
13, 30311–30348, 2013

Kaolinite particles as ice nuclei

H. Wex et al.

Title Page
Abstract | Introduction
Conclusions | References
Tables | Figures
◀| |▶
◀ ▶
Back | Close
Full Screen / Esc
Printer-friendly Version
Interactive Discussion

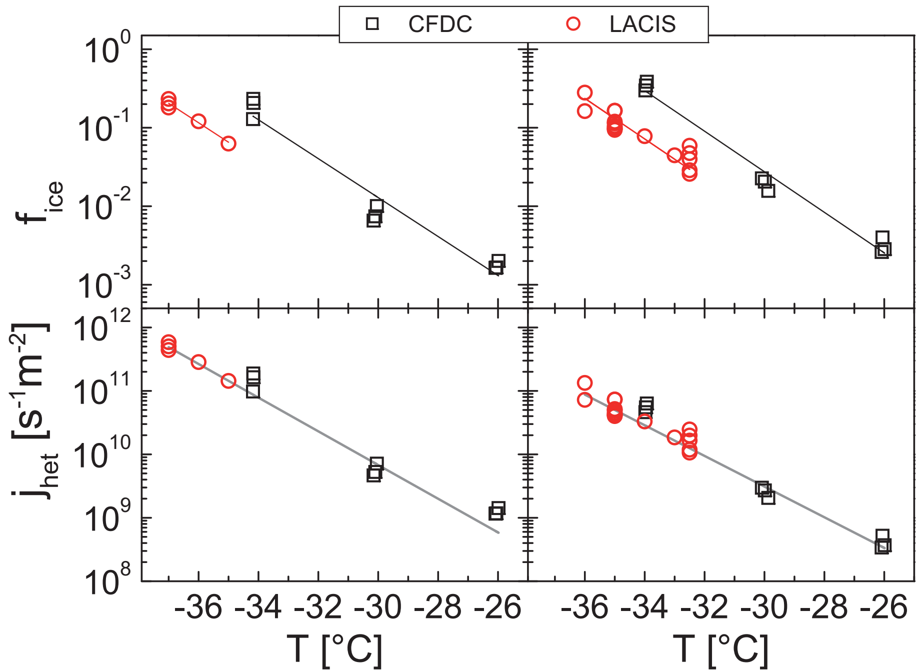

Fig. 2. Measured f_{ice} and derived j_{het} for CFDC and LACIS for two particle types (left panels: 300 nm Fluka kaolinite coated with LG at 80 °C; right panels: 700 nm Fluka kaolinite (no coating)).

ACPD
13, 30311–30348, 2013

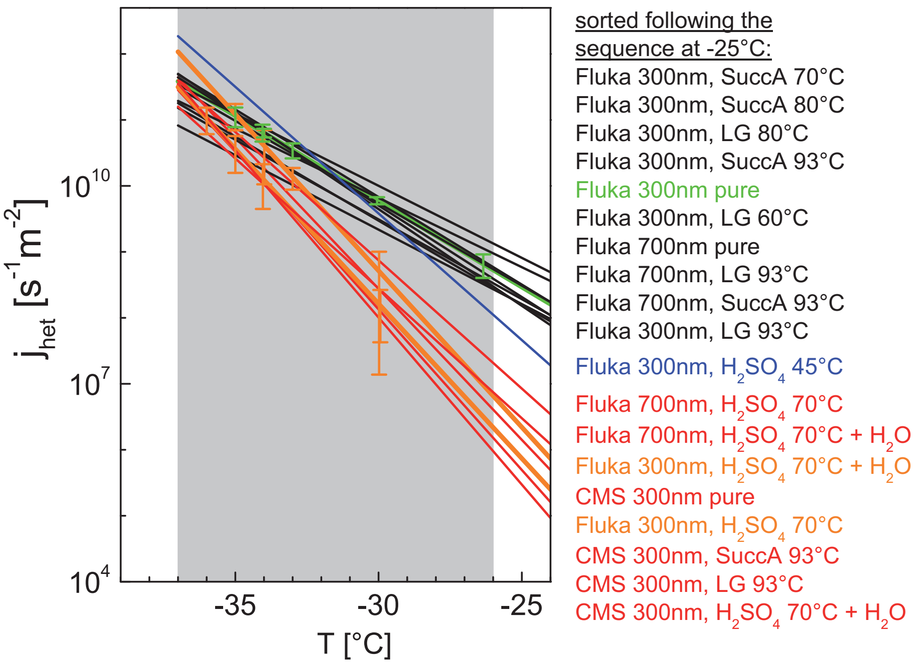

Fig. 3. Fitting curves for j_{het} for the different particle types, following Eq. (2). Corresponding values of the fit parameters A and B are shown in Fig. 4. j_{het} for pure Fluka kaolinite particles is shown in green, while black lines show j_{het} for these particles coated with SuccA or LG. Red and orange lines depict j_{het} for all CMS kaolinite particles and for all particles coated with H_2SO_4 at a coating temperature of 70 °C. Error bars are given exemplarily for the green and the two orange lines.

ACPD
13, 30311–30348, 2013

Kaolinite particles as ice nuclei

H. Wex et al.

ACPD
13, 30311–30348, 2013

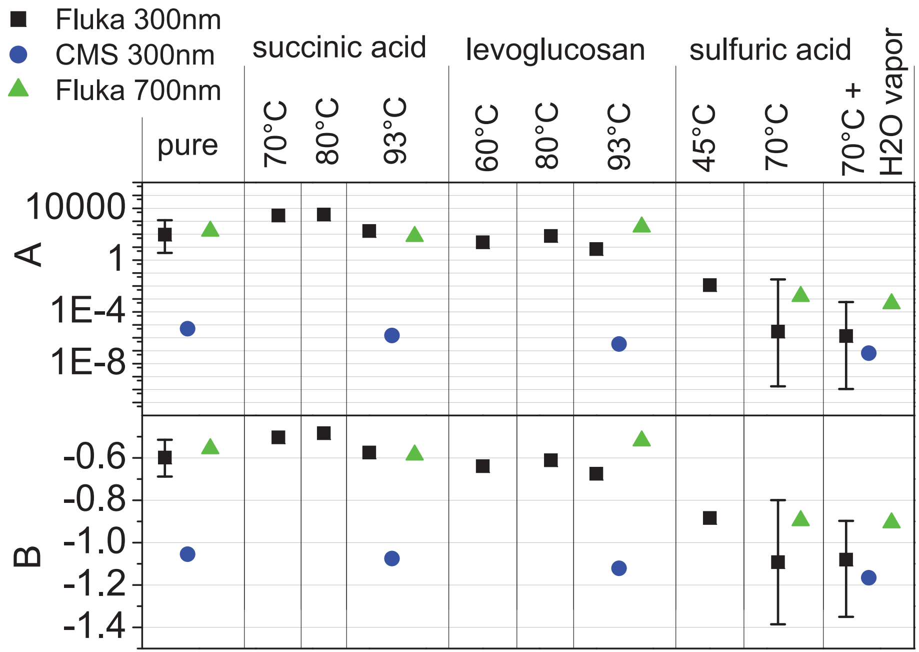

Fig. 4. Overview over fit parameters A and B for j_{het} for the different particle types. Error bars are given for the same datasets for which they were shown in Fig. 3.

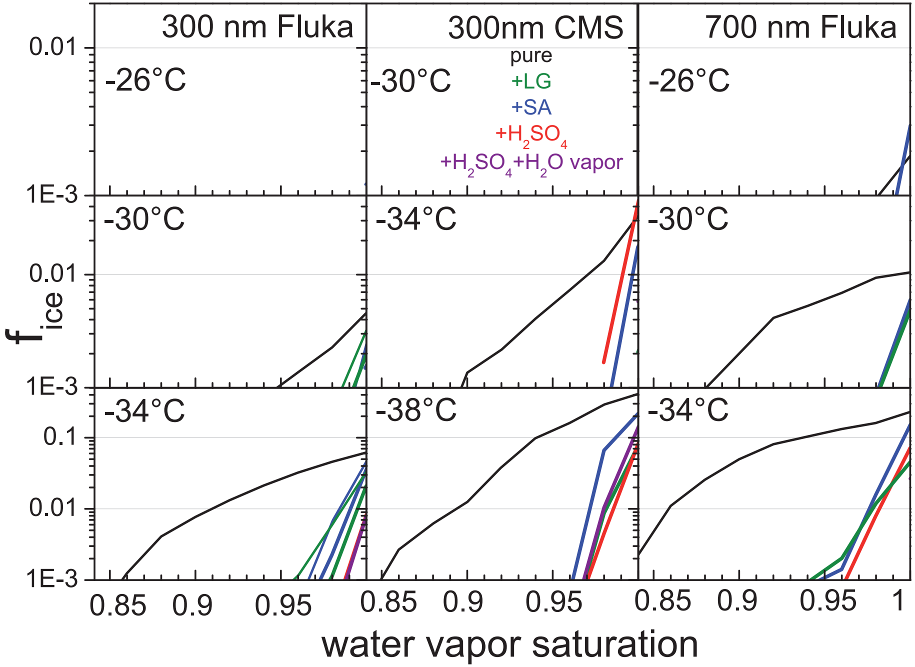

Fig. 5. f_{ice} measured with the CFDC for $S_w < 1$. Thinner lines indicate medium thick coatings, thicker lines represent thick coatings. The type of coating is indicated by colors, the color coding can be seen in the upper middle panel.

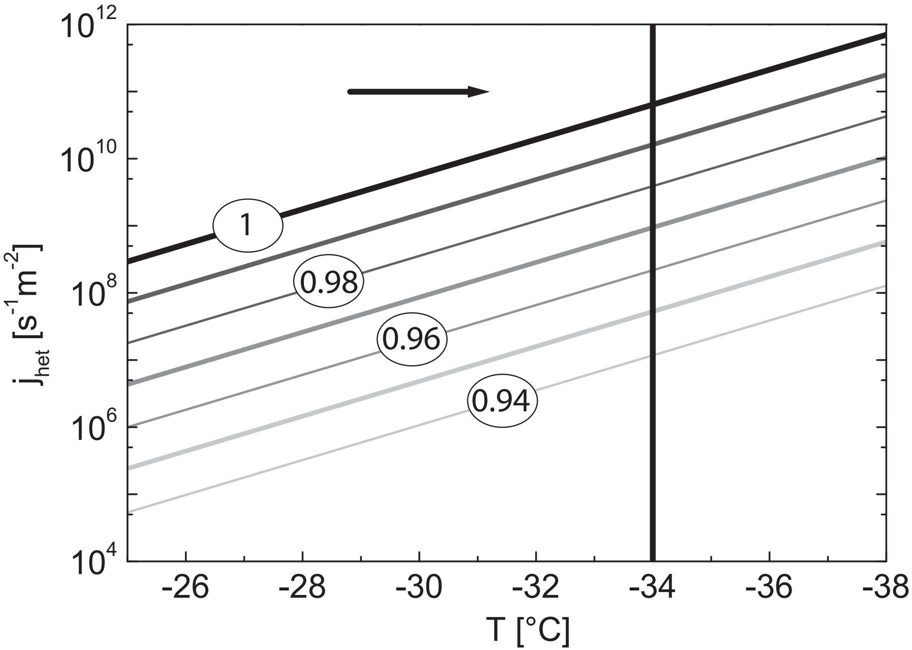

Fig. 6. j_{het} estimated for different water activities a_w in a solution droplet surrounding a particle. The black line is the one for the uncoated 300 nm Fluka kaolinite particles. The different grey lines indicate the curves for j_{het} for such particles immersed in a solution with $0.94 \le a_w \le 0.99$ (values indicated on every other line).

ACPD
13, 30311–30348, 2013

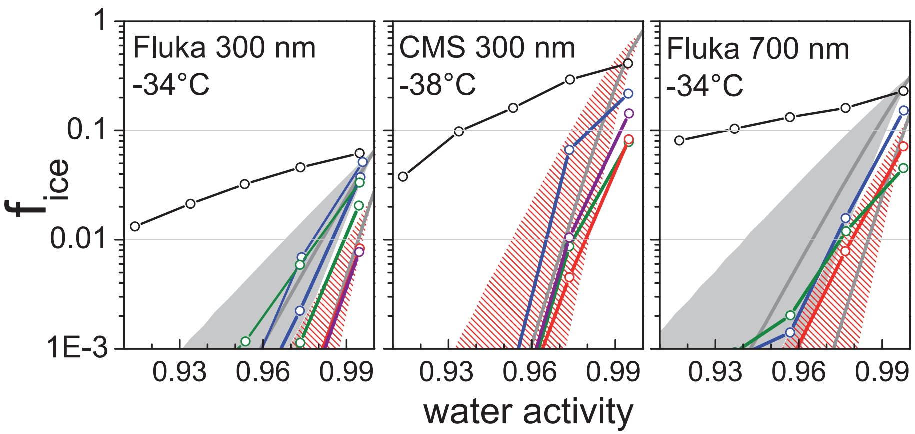

Fig. 7. Measured f_{ice} for deposition ice nucleation and expected ice nucleation behavior for particles which are completely coated by a solution (grey areas for pure Fluka kaolinite or this kaolinite coated with SuccA or LG, and redly striped areas for CMS kaolinite and Fluka kaolinite coated with H_2SO_4). The color code for the measured data with respect to the type of coating is similar to that used in Fig. 5.

ACPD
13, 30311–30348, 2013

Kaolinite particles as ice nuclei

H. Wex et al.

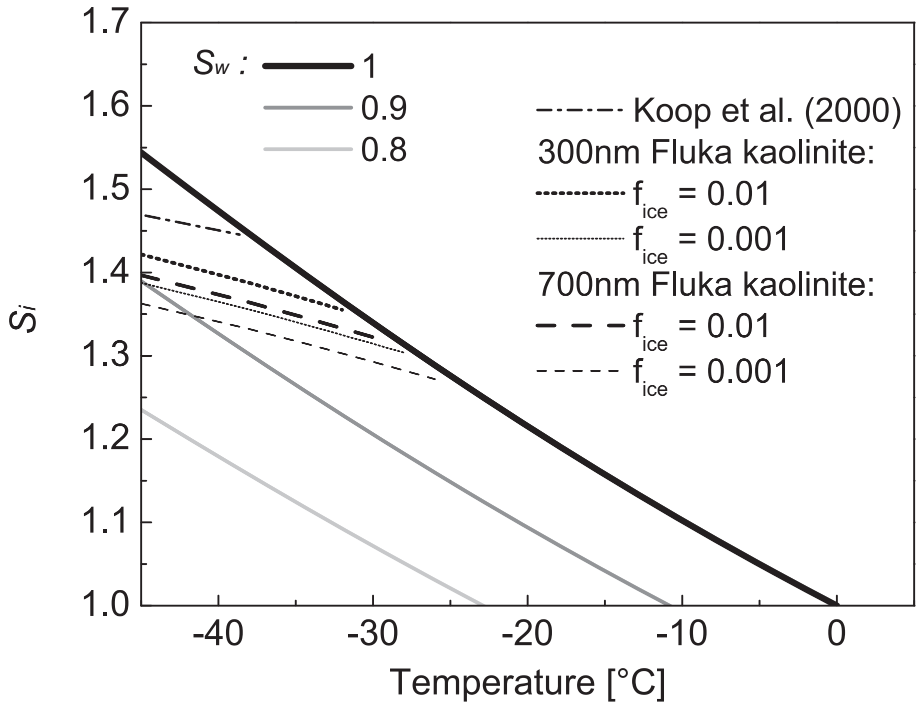

Fig. 8. The plot shows the relation between the water vapor saturation ratio above ice (S_i) to that above water S_w. Lines are shown for S_w of 0.8, 0.9 and 1. Also shown is a line for homogeneous freezing taken from Koop et al. (2000) and lines indicating an f_{ice} of 1 % and 0.1 % for the 300 and 700 nm particles with LG and SuccA coating examined in this study.

ACPD
13, 30311–30348, 2013

Kaolinite particles as ice nuclei

H. Wex et al.